Spatiotemporal distributions of dissolved N_2O concentration, diffusive N_2O flux and relevant functional genes along a coastal creek in southeastern China

Ping Yang[a,b,c,d*], Yongxin Lin[a,b], Hong Yang[e], Chuan Tong[a,c,d], Linhai Zhang[a,b,c,d], Derrick Y. F. Lai[f], Dongyao Sun[g*], Lishan Tan[f], Lele Tang[a], Yan Hong[a], Kam W. Tang[h*]

[a]*School of Geographical Sciences, Fujian Normal University, Fuzhou 350007, P.R. China*

[b]Fujian Provincial Key Laboratory for Subtropical Resources and Environment, Fujian Normal University, Fuzhou 350117, P.R. China

[c]*Research Centre of Wetlands in Subtropical Region, Fujian Normal University, Fuzhou 350007, P.R. China*

[d]*Fujian Minjiang Estuary Wetland Ecosystem National Observation and Research Station，National Forestry and Grassland Administration, Fuzhou 350215, China*

[e]Department of Geography and Environmental Science, University of Reading, Reading, UK

[f]Department of Geography and Resource Management, The Chinese University of Hong Kong, Shatin, New Territories, Hong Kong SAR, China

[g]School of Geography Science and Geomatics Engineering, Suzhou University of Science and Technology, Suzhou 215009, China

[h]Department of Biosciences, Swansea University, Swansea SA2 8PP, U. K.

*Corresponding author:

22 yangping528@sina.cn (P. Yang); dongyaos@126.com (D.Y. Sun);
23 k.w.tang@swansea.ac.uk (K.W. Tang)

A B S T R A C T

Increased anthropogenic input of nitrogen into coastal creeks make them potential hotspots for N_2O production and emission, but they are often excluded from regional and global N_2O budget, and high-resolution sampling is required to characterize the strong spatiotemporal heterogeneity within the creeks. In this study, we analyzed the N_2O concentration and diffusive N_2O flux within a coastal creek in the Shanyutan Wetland in southeastern China in high spatial resolution across four seasons. Ancillary hydrographical variables and N_2O-related functional gene abundances were also measured. Results showed that the creek was consistently oversaturated in N_2O, at a seasonal average of 5.6-14.2 nmol L^{-1}, relative to the overlying atmosphere. The spatial distribution of N_2O followed the gradient of nitrogenous substrate but was inversely related to the salinity gradient, and the coefficient of spatial variation of N_2O flux ranged from 66.3% to 116.5%. Nitrite reduction (based on *nirK* and *nirS* gene abundances) and ammonia oxidation (*AOA amoA* and *AOB amoA*) appeared to outpace N_2O reduction (*nosZ I* and *nosZ II*), and these were the main microbial processes that determined N_2O concentration and flux. Both N_2O concentration and flux were substantially higher in autumn than those in the other seasons, but that did not appear to be related to precipitation. N_2O diffusive flux from the creek averaged 322.2 nmol m^{-2} h^{-1}, which was over 2 times higher than the global average for lakes and reservoirs. Our results highlight that coastal creeks are strong atmospheric N_2O sources with high spatiotemporal variability.

Keywords: Tidal creeks; Nitrous oxide (N_2O); Spatiotemporal variation; Wastewater discharge; Coastal wetland

List of abbreviations:

N_2O, nitrous oxide; C_{N2O}, dissolved N_2O concentration; F_{N2O}, diffusive N_2O flux; DO, dissolved oxygen; T_W, water temperature; TN, total dissolved nitrogen; NH_4^+-N, ammonia nitrogen; NO_3^--N, nitrate nitrogen; PLS-SEM, Partial least square structural equation modeling.

1. Introduction

The greenhouse gas nitrous oxide (N_2O) not only contributes to global warming, but it also depletes stratospheric ozone (Ravishankara et al., 2009; Bahram et al., 2022). In 2022, the global mean concentration of atmospheric N_2O reached 335.8 ppbv (WMO, 2023), exceeding the pre-industrial level by ~24%. Microbial nitrification and denitrification within soil and water are the main N_2O production processes in nature (Beaulieu et al., 2015; Maher et al., 2016; Toyoda et al., 2016; Hutchins and Capone, 2022). Approximately 20% of the global N_2O emission is believed to originate from marine habitats (Tian et al., 2020), of which ~60% is from the coastal regions (Bange et al., 1996).

Coastal wetlands play key roles in nitrogen cycling (Bowden, 1986; Murray et al., 2015; Plummer et al., 2015; Wang et al., 2018) thanks to their high accretion rate and organic deposition (Chmura et al., 2003; Cloern et al., 2016; Zhang et al., 2016; Schulz et al., 2023). Many coastal wetlands are irrigated by creeks that channel materials (e.g., water, nutrients, sediments, etc.), energy and information across the land (Green and Hancock, 2012; Pieterse et al., 2016; Wu et al., 2020). Waste discharge from domestic, farming and industrial activities upstream often leads to an elevated nitrogen level within these creeks (Lu et al., 2023; Sanger et al., 2015; Wessel et al., 2022), making them potential hotspots for N_2O production and emission. Different functional microbial communities may drive N_2O production (Bahram et al., 2022; Yang et al., 2023; Zhou et al., 2023), but the relevant data for coastal creeks are rare.

Despite its relatively small areal coverage, a meandering creek running across a wetland is subject to varying degrees of fresh- and salt-water input, sedimentation, biological and ecological activities along its length, creating a heterogeneous and biogeochemically active

micro-geomorphological feature (Sanderson et al., 2000; Vandenbruwaene et al., 2016; Wu et al., 2020). Low-resolution spatial sampling commonly done in the literature therefore may not be sufficient to properly characterize these highly heterogeneous systems (e.g., Barnes et al., 2006; Ferrón et al., 2007; Maher et al., 2016; Tan et al., 2021).

We conducted high spatial resolution sampling in a coastal creek in the Shanyutan Wetland in southeastern China over four seasons, including dissolved N_2O concentration, diffusive N_2O flux, relevant microbial functional gene abundances, and ancillary hydrographical variables. The aim was to characterize the biological and environmental drivers of spatiotemporal distributions of N_2O along the creek. We hypothesized that N_2O distribution and emission were highly heterogeneous in time and in space within the creek, and that coastal creeks play an important role in N_2O emissions on a per unit area basis.

2. Materials and methods

2.1. Study area and water sampling

This research took place in a coastal creek (Figure 1c) within the Shanyutan Wetland of southeastern China (coordinates: 26°00′36″N to 26°03′42″N, 119°34′12″E to 119°41′40″E; Figure 1b). The dominant vegetation includes *Phragmites australis*, *Scirpus triqueter* and *Cyperus malaccensis*. The region is influenced by a subtropical monsoonal climate, characterized by an average yearly air temperature of 19.6 ºC and annual rainfall of 1,350 mm (Yang et al., 2021a). The creek is 4.05 km long and 50-150 m wide, with an average diurnal tidal range of 2.5–6.0 m. Substantial quantities of organic matter and nutrients are channeled into the creek from upstream through embankments equipped with sluices (Figure 1c).

Field sampling was conducted on 22nd October 2022 (autumn), 23rd February 2022

(winter), 23rd April 2023 (spring) and 21st June 2023 (summer). All the sampling work was done between 8:00 a.m. and 10:00 a.m. at flood (slack) tide when the water depth was sufficiently deep to navigate through and water flow was minimal. A total of 27 sites at an interval of ~150 m were sampled in each of the seasons. At each site, water sample from 20-cm depth was collected in triplicates using 150-mL polyethylene bottles for measuring total dissolved nitrogen (TN), NO_3^--N and NH_4^+-N and N_2O-related functional gene abundances. To measure dissolved N_2O concentration, additional triplicate water samples were taken at each site using a syringe fitted with a three-way valve into 55-mL pre-evacuated air-tight serum glass bottles (Tan et al., 2021). Atmospheric gas samples were also collected at each location and stored in 50 mL aluminum-foil bags for gas sampling (Dalian Delin Gas Packing Co., Ltd., China). These samples were transported back to the laboratory in a cooler within 4-6 h and analyzed within 72 h.

2.2. Physical and chemical measurements

At each site, we measured at 20-cm depth the water temperature (T_W) and dissolved oxygen (DO) with a multiparameter probe (550A YSI, USA), salinity with a salinity meter (Eutech Instruments-Salt6, USA), and pH with a pH meter (Orion-868, USA).

In the laboratory, water subsamples were passed through 0.45-μm cellulose acetate filters (Biotrans™ nylon membranes), and the filtrates were analyzed for TN, NH_4^+-N and NO_3^-N using a flow injection analyzer (Skalar Analytical SAN^{++}, The Netherlands). The detection limits for TN, NH_4^+-N and NO_3^-N were 3.0, 0.6 and 0.6 μg L^{-1}, respectively; the relative standard deviation ranged from 2.0% to 3.0%.

2.3. DNA extraction and quantitative PCR

We filtered 100 mL of each water sample through a 0.22-μm cellulose nitrate membrane. Afterward, we used the FastDNA™ Spin Kit for Soil (MP Biomedicals, USA) to extract DNA from the membrane, following the manufacturer's instructions. DNA quantity and quality were checked using a NanoDrop spectrophotometer (Thermo Fisher Scientific, USA).

The CFX384 Optical Real-Time Detection System (Bio-Rad Laboratories Inc., Hercules, CA, USA) was used to measure the essential functional genes for N_2O dynamics, including those responsible for nitrite reduction (*nirK*, *nirS*), ammonia oxidation (AOA *amoA*, AOB *amoA*), and the reduction of nitrous oxide (*nosZ* I and *nosZ* II). Standard curves were obtained by employing plasmid DNA from a single representative clone that carried each specific gene. In every reaction, the 10 μl mixture contained 5 μl of SYBR qPCR master mix (Vazyme, China), 0.25 μl for each primer utilized, and 1 μl of the DNA template (approximately 1–10 ng of DNA). Sterilized distilled water was run as the negative control. Details of the gene-specific primers and thermal settings are shown in Table S1. Amplification consistently produced a single peak, and the efficiency of amplification ranged from 80% to 102%, accompanied by R^2 values spanning from 0.993 to 0.999.

2.4. Measurement of N_2O concentrations

The concentrations of dissolved N_2O (C_{N2O}) were determined via the headspace equilibration technique (e.g., Davidson et al., 2015; Zhang et al., 2023). Briefly, subsurface water at 20-cm depth was collected bubble-free with a syringe, immediately placed into 55-mL pre-evacuated serum glass bottles, which were then sealed airtight. Afterward, approximately ~0.5 mL of saturated $HgCl_2$ solution was added to stop microbial processes (Davidson et al., 2015; Liang et al., 2023). In the laboratory, nitrogen gas (>99.999% purity) was injected into

each bottle to displace 25 mL of the water. The bottles were shaken on an oscillator (IS-RDD3, China) for 10 min to facilitate an equilibrium between the gaseous and liquid phases (Yang et al., 2022a). After a 30-min delay, 5 ml of the headspace gas was extracted with a syringe and injected into a Shimazu GC-2014 gas chromatograph (Kyoto, Japan) fitted with an electron capture detector to measure N_2O. Atmospheric gas samples collected on site were injected directly into the gas chromatograph. The *in situ* dissolved N_2O concentration (nmol L^{-1}) was calculated from the measured headspace N_2O concentration and the Bunsen solubility coefficient for N_2O based on temperature and salinity (Weiss and Price, 1980; Yang et al., 2022a). Saturation of N_2O (S_{N2O}, %) in the creek's surface water was calculated as:

$$S_{N2O} = C_W / (\alpha \times C_A) \times 100\% \quad (1)$$

where C_{N2O} was the measured concentration of dissolved N_2O (C_{N2O}, nmol L^{-1}) in the surface water; C_A was the concentration of atmospheric N_2O (nmol L^{-1}) at the sampling site; α was the Bunsen coefficient.

2.5. Calculations of water-to-air diffusive N_2O fluxes

Diffusive N_2O fluxes (F_{N2O}, nmol m^{-2} h^{-1}) were calculated from the thin boundary-layer model (Liss and Slater, 1974; Que et al., 2023), based on the water-air N_2O concentration gradient and the N_2O transfer velocity (Liang et al., 2023; Musenze et al., 2014; Wang et al., 2020), as follows:

$$F_{N2O} = k_x \times (C_{water} - C_{eq}) \quad (2)$$

where C_{water} was the measured concentration of dissolved N_2O (C_{N2O}, nmol L^{-1}) in the surface water; C_{eq} was the concentration of dissolved N_2O (nmol L^{-1}) at equilibrium with the atmosphere calculated from the on-site atmospheric N_2O concentration and Bunsen coefficient.

k_x was the transfer velocity of N_2O (m h^{-1}) based on the model of Raymond and Cole (2001) because of their study environment (estuary) being the most comparable to our coastal creek:

$$k_x = 1.91e^{0.35U_{10}} \times (Sc/600)^{-1/2} \quad (3)$$

where U_{10} was the wind velocity at a 10 meter height above the creek (m s^{-1}) devoid of friction effects (Crusius and Wanninkhof, 2003). *Sc* was the Schmidt number for N_2O calculated as (Wanninkhof, 1992):

$$Sc_{N2O} = 2301.1 - 151.1t + 4.7364t^2 - 0.059431t^3 \quad (4)$$

where *t* was the temperature of the surface water (°C).

2.6. Statistical analysis

Two-way analysis of variance (ANOVA) was conducted in SPSS 25.0 (IBM, Armonk, NY, USA) to test for the effects of sampling locations, seasons and their interactions on various environmental variables, dissolved N_2O concentration and N_2O diffusive flux. Significant differences in various functional genes abundances over seasons were tested using Kruskal-Wallis test ~~non parametric methods~~. The relationships among the different variables were explored using Spearman correlation analysis in the R vegan package (R Foundation for Statistical Computing, 2013). Redundancy analysis (RDA) was conducted using CANOCO 5.0 (Microcomputer Power, Ithaca, USA) to assess the relative influence of different environmental parameters on dissolved N_2O concentration and N_2O diffusive flux. Partial least square structural equation modeling (PLS-SEM) was employed using the R 'semPLS' package (R Foundation for Statistical Computing, 2013) to identify the direct or indirect influences of different environmental variables on dissolved N_2O concentration and N_2O diffusive flux. Spatial interpolation of field data was done using the Kriging method in the software ArcGIS

Commented [1]: Dr Yang can you specify which test(s)?
回复： Tang 老师，我用的是非参数检验中的独立样本(I)检验，该种方法在英文中该如何表达？

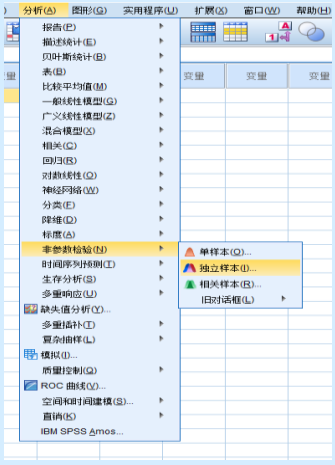

Commented [KT2R1]: Dear Dr. Yang, for independent sample non-parametric test, it is usually Mann-Whitley test when comparing two groups, and Kruskal-Wallis test when comparing more than 2 groups. Because you have more than 2 groups, I guess it is Kruskal-Wallis.

10.2 (ESRI Inc., Redlands, CA, USA). Results were reported as the average ± standard error (SE), unless specified differently. A significance level of $p < 0.05$ was applied for all statistical evaluations.

3. Results

3.1. Spatiotemporal distributions of N_2O

The concentrations of N_2O in the creek's surface water (C_{N2O}) exhibited significant spatial variability, with the coefficient of variation ranging from 28.3% to 105.1%. Overall, the mean C_{N2O} in the creek was significantly higher near the sluice gate, and decreased significantly toward the sea ($p<0.001$; Figure 2a–d). C_{N2O} also varied significantly between seasons ($F_{df=3}=7.927$, $p<0.001$). The seasonal average C_{N2O} varied between 5.6 ± 0.3 nmol L^{-1} and 14.2 ± 2.5 nmol L^{-1}, with the highest concentration recorded in autumn, followed by summer, winter and spring (Figure 3a).

Across all seasons and sites, the surface water was oversaturated in dissolved N_2O relative to the air (Figure S1), making the creek a net source of atmospheric N_2O. The diffusive N_2O flux (F_{N2O}) varied between 6.6 nmol m^{-2} h^{-1} and 2698.6 nmol m^{-2} h^{-1}, and averaged 322.2 ± 163.8 nmol m^{-2} h^{-1} throughout the study.

Similar to C_{N2O}, F_{N2O} exhibited remarkable spatial variations, with highest values near the sluice gate and it decreased along the creek toward the sea (Figure 2e–h). Seasonally, the highest F_{N2O} was observed in autumn with a mean value of 813.4 ± 182.4 nmol m^{-2} h^{-1} (Figure 3b), which was more than four times higher than the other seasons ($F_{df=3}=12.578$, $p<0.001$).

3.2. Nitrogenous substrates and functional gene abundances

The spatial data on nitrogenous substrates (TN, NH_4^+-N and NO_3^--N) and abundances of

functional genes related to N_2O dynamics (AOA *amoA*, AOB *amoA*, *nirK*, *nirS*, *nosZ* I, and *nosZ* II) in the creek's surface water are shown in Figure 4 and Figure 5, respectively. Both the concentrations of nitrogenous substrates and copy numbers of functional genes decreased along the direction from land to sea in all four seasons.

The seasonal variations in nitrogenous substrates concentrations and functional gene abundances during the study period are shown in Table 1 and Table 2. TN, NH_4^+-N and NO_3^--N concentrations decreased in the order of autumn > spring > winter > summer (Table 1). For N_2O-related functional genes, we observed generally higher AOA *amoA*, AOB *amoA* and *nosZ* II in winter ($p<0.05$ or <0.01; Table 2), and higher *nirK*, *nirS*, *nosZ* I in autumn and winter ($p<0.05$ or <0.01; Table 2).

3.3. Physicochemical properties of surface water

The physicochemical characteristics of the creek's surface water varied by location and season (Figure S2). While T_W and pH showed no significant variation across the different sampling locations ($p>0.05$), DO concentration and salinity increased noticeably along the creek from land to sea.

Across the four seasons, T_W was highest in summer (30.4 ºC), followed by autumn (22.1 ºC), spring (21.3 ºC) and winter (12.6 ºC) (Figure S2). We observed generally higher DO in winter (8.4 mg L^{-1}) and spring (8.5 mg L^{-1}), and higher salinity in winter (8.8‰) (Figure S2). The mean pH did not show significant seasonal variation ($p>0.05$; Figure S2).

3.4. Environmental drivers of N_2O concentration and diffusive flux

C_{N2O} and F_{N2O} correlated positively with T_W, nitrogenous substrates and N_2O-related functional gene abundances ($p<0.01$), but negatively with DO and salinity ($p<0.01$) (Table S2).

pH did not correlate significantly with either C_{N2O} or F_{N2O} (Table S2).

We used RDA and PLS-SEM analyses to identify the main environmental drivers of the spatiotemporal variations in C_{N2O} or F_{N2O}. Overall, environmental parameters explained 96.1% of the variances in C_{N2O} or F_{N2O} among all data (Figure 6a). *nirS*, nitrogenous substrates and salinity together explained 87.6% of the variations (Figure 6b). According to PLS-SEM analysis, C_{N2O} was influenced positively by *nirS* and NO_3^--N and negatively by salinity (Figure 7a); *nirS* had the largest magnitude of influence on C_{N2O} and F_{N2O} (Figure 7b).

4. Discussion

4.1. Coastal creek as an atmospheric N_2O source

The surface water was oversaturated in N_2O relative to the atmosphere along the entire creek, making it a net source of atmospheric N_2O (Figure S1). N_2O diffusive flux from the creek ranged from 6.6 to 2698.6 nmol m^{-2} h^{-1} with a mean of 322.2 nmol m^{-2} h^{-1} (Figure 3b), which was substantially lower than that observed in salt marshes (629.5–3947.8 nmol m^{-2} h^{-1}; Wang et al., 2018; Yang et al., 2022b) and the nearby aquaculture ponds (975.0 nmol m^{-2} h^{-1}; Yang et al., 2022b). However, it was much higher than that from mangrove wetlands (e.g., Wang et al., 2015; Murray et al., 2018; Comer-Warner et al., 2022; Ma et al., 2023) and eutrophic estuaries in the temperate and subtropical regions (Burgos et al., 2017; Li et al., 2022; Huertas, 2018; Wells et al., 2018; Sturm et al., 2017). More broadly, the average N_2O flux from our creek was over 2 times higher than the global mean value for lakes and reservoirs in the tropical and polar regions (Hu et al., 2016). Similar to previous findings (e.g., Barnes et al., 2006; Ferrón et al., 2007; Tan et al., 2021), our results suggest that coastal creeks are strong N_2O emitters per unit area, but they are often excluded from regional and global N_2O budgets.

4.2. Spatial distributions of N_2O and relevant microbial processes

Microbial production of N_2O *in situ* can be stimulated by the supply of substrates (Bahram et al., 2022; Li et al., 2021; Yang et al., 2023), subsequently increasing N_2O emission to the atmosphere (Amaral et al., 2021; Liang et al., 2023; Xiao et al., 2019a; Yang et al., 2021b). Soil N_2O production alongside the creek can also be influenced by vegetation types, adding to the spatial variability in dissolved N_2O along the creek (Chen et al., 2007; Espenberg et al., 2024). Our high-resolution sampling revealed a strong spatial heterogeneity in N_2O concentration, % saturation and flux along the creek (Figure 2). N_2O concentration tended to be higher upstream matching the spatial distribution of nitrogenous substrates (Figure 4), similar to the findings in estuaries (Amaral et al., 2021; Huertas et al., 2018; Liu et al., 2022; Xiang et al., 2023), and was likely caused by waste discharge through the sluice gate at the head of the creek. Some previous studies sampled only one or a few fixed points along a creek (e.g., Barnes et al., 2006; Ferrón et al., 2007; Maher et al., 2016; Tan et al., 2021), which would have mischaracterized the true extent of N_2O production and emission, especially in creeks strongly influenced by terrestrial discharge.

Nitrite reduction and ammonia oxidation are two important steps in microbial production of N_2O (Bahram et al., 2022; Kozlowski et al., 2014; Zhou et al., 2023). While we did not have *in situ* N_2O production data, we may use the abundances of the relevant function genes (AOA *amoA* and AOB *amoA* for ammonia oxidation; *nirK* and *nirS* for nitrite reduction) as proxies (Figure 5a-p). Overall, their spatial distributions along the creek tracked the distributions of nitrogenous substrates quite closely (Figure 4). Nitrite reduction is favored in low-oxygen environment (Murray et al., 2015; Venterea et al., 2007); therefore, it is no surprise that higher

abundances of *nirK* and *nirS* genes were found upstream where DO was substantially lower (Figure S2b). Both ammonia oxidizing bacteria (AOB) and ammonia oxidizing archaea (AOA) can produce N_2O from NH_3 (Prosser et al., 2020). While it may seem counterintuitive that *amoA* gene abundances were higher in the low-oxygen part of the creek (Figure 5a-h), both field and laboratory studies by others have shown that N_2O production via ammonia oxidation actually increased when dissolved oxygen decreased to near anoxia (Prosser et al., 2020; Zhu-Barker et al., 2013). Between nitrite reducers and ammonia oxidizers, our RDA and PLS-SEM analyses suggested that the former played a much stronger role in determining N_2O production along the creek (Figures 7, 8).

Conversely, microbial reduction of N_2O to N_2 could decrease N_2O in the water, and the process is driven by enzymes encoded by *nosZ I* and *nosZ II* genes. Because this enzymatic process is favored by low-oxygen condition, the spatial distributions of *nosZ* genes (Figure 5q-x) also followed the distribution of DO and were strongly correlated to N_2O (Table S2). Despite the fact that the copy numbers of the *nosZ* genes were of similar magnitudes to the genes for N_2O production, the large accumulation of dissolved N_2O upstream suggests that microbial N_2O production rate still outpaced N_2O reduction rate.

The coastal creek was directly affected by terrestrial freshwater discharge on one end and saltwater intrusion on the other, creating a salinity gradient along the creek (Figure S2d). Other studies have shown that high salinity induces ionic stress (Chambers et al., 2013; Neubauer et al., 2013) or inhibits microbial and enzymatic activities (Francis et al., 2003; Wang et al., 2010; Yang et al., 2022b), thereby reducing N_2O production from sediment and water column (Rysgaard et al., 1999; Xiang et al., 2023; Wang et al., 2018) and subsequent emission. Likewise,

our results showed a significantly negative correlation between N_2O concentration (and flux) and salinity (Table S2). The abundance of microbial functional genes (Figure 5) and salinity (Figure S2d) also showed opposite spatial gradients. These observations suggest that salinity played a key role in regulating N_2O biogeochemical processes in the coastal creek, as was confirmed by our PLS-SEM analysis (Figure 7).

4.3. Temporal distributions of N_2O flux and their regulating factors

N_2O diffusive flux from the creek exhibited distinct seasonal variations, with a substantially higher emission in the autumn (Figure 3b). Although previous studies have shown a positive correlation between temperature and N_2O production in aquatic systems (Tian et al., 2017; Hinshaw and Dahlgren, 2013; Yang et al., 2021b; Shrestha and Wang, 2018), we found that water temperature had an insignificant effect on N_2O concentration and flux (Table S2). This perhaps reflects the fact that nitrogenous substrate availability outweighed the effect of water temperature (Xiao et al., 2019b; Davidson et al. 2015; Capodici et al., 2018), similar to observations in other water bodies under strong anthropogenic influences (Xiao et al., 2019b; Audet et al., 2017; Hama-Aziz et al., 2017).

Some researchers suggested that intense rainfall may lead to an increased transfer of nutrients and greenhouse gases from the catchment to the water bodies (Xiao et al., 2021; Einola et al., 2011; Sinha et al., 2017; Dinsmore et al., 2013), with the consequence of increasing microbial greenhouse gas production and subsequent emissions (Natchimuthu et al., 2014; Yu et al., 2017; Stanley et al., 2016). To explore this possibility, we used precipitation data from an automated weather station situated at the Min River Estuary as a part of the China Wetland Ecosystem Research Network, and plotted it against N_2O concentration and flux, which showed

opposite relationships to what was expected (Figure S3). Therefore, we posit that higher precipitation may have diluted the substrates (Figure 4) and microbes (Figure 5) that drove *in situ* biogeochemical reactions, similar to observations in riverine (He et al., 2017) and lentic systems (Holgerson, 2015; Outram and Hiscock, 2012.Yang et al., 2021b).

5. Conclusions and recommendations

A recent synthesis study has raised the estimate of global contribution of N_2O emission from coastal waters (Tian et al., 2020). However, the global N_2O budget remains highly uncertain due to the limited types of systems being studied and low data resolution. Along with previous findings (Barnes et al., 2006; Ferrón et al., 2007; Tan et al., 2021), this study showed that coastal creeks are important habitats for N_2O production and emission, and should be included in the regional and global N_2O budget. Meanwhile, our data revealed a strong spatial heterogeneity in N_2O concentration and flux (coefficient of variation 66.3–116.5%) as well as distinct seasonal variations. As such, low-resolution sampling in space and in time would grossly mischaracterize N_2O contributions from coastal creeks, especially those under strong anthropogenic influences.

While our data showed that the coastal creek was a strong N_2O emitter, we may have underestimated the magnitude of N_2O emission for several reasons. The water level in the creek was influenced by the tidal cycle. Due to logistical constraints, we were only able to do our field sampling at high water during the day. The literature has shown that release of N_2O from sediment is stronger at low tide when hydrostatic pressure drops (Barnes et al., 2006). Similarly, some researchers observed higher N_2O emission from rivers at night than in the day (Laursen and Seitzinger, 2004). Therefore, our measurements may have underestimated N_2O emission

from the creek. Additional sampling during low-water and at night would further improve the spatial and temporal resolutions of N_2O distribution within the creek.

In addition to N_2O, the substrate-rich, low salinity and low oxygen conditions especially upstream may also promote methanogenesis. However, denitrifiers and methanogens may compete against each other for electron donors (Achtnich et al., 1995), and some research has shown anaerobic methane oxidation coupled with nitrite reduction as a methane sink in coastal environments (Shen et al., 2016). While we did not collect methane data in the present study, this inhibitory effect on methanogenesis, if proven, may partially mitigate the overall climate impact of the creek.

Declaration of competing interest

The authors declare that they have no known competing financial interests or personal relationships that could have appeared to influence the work reported in this paper.

Acknowledgements

The study received collaborative financial support from the National Natural Science Foundation of China (Grant No. 41801070), Natural Science Foundation of Fujian Province (No. 2022R1002006) and Minjiang Scholar Programme.

References

Achtnich, C., Bak, F., Conrad, R., 1995. Competition for electron donors among nitrate reducers, ferric iron reducers, sulfate reducers, and methanogens in anoxic paddy soil. Biol. Fert. Soils, 19, 65–72. https://doi.org/10.1007/bf00336349.

Amaral, V., Ortega, T., Romera-Castillo, C., Forja, J., 2021. Linkages between greenhouse

gases (CO_2, CH_4, and N_2O) and dissolved organic matter composition in a shallow estuary. Sci. Total Environ. 788, 147863. https://doi.org/10.1016/j.scitotenv.2021.147863.

Audet, J., Wallin, M.B., Kyllmar, K., Andersson, S., Bishop, K., 2017. Nitrous oxide emissions from streams in a Swedish agricultural catchment. Agr. Ecosyst. Environ. 236, 295–303. https://doi.org/10.1016/j.agee.2016.12.012.

Bahram, M., Espenberg, M., Pärn, J., Lehtovirta-Morley, L., Anslan, S., Kasak, K., Kõljalg, U., Liira, J., Maddison, M., Moora, M., Niinemets, Ü., Öpik, M., Pärtel, M., Soosaar, K., Zobel, M., Hildebrand, F., Tedersoo, L., Mander, Ü., 2022. Structure and function of the soil microbiome underlying N_2O emissions from global wetlands. Nat. Commun. 13, 1430. https://doi.org/10.1038/s41467-022-29161-3.

Bange, H.W., Rapsomanikis, S., Andreae, M.O., 1996. Nitrous oxide in coastal waters. Global Biogeochem. Cy. 10, 197–207. https://doi.org/10.1029/95GB03834.

Barnes, J., Ramesh, R., Purvaja, R., Nirmal Rajkumar, A., Senthil Kumar, B., Krithika, K., Ravichandran, K.,Uher, G., Upstill-Goddard, R., 2006. Tidal dynamics and rainfall control N_2O and CH_4 emissions from a pristine mangrove creek. Geophys. Res. Lett. 33, L15405. https://doi.org/10.1029/2006GL026829.

Beaulieu, J.J., Nietch, C.T., Young, J.L., 2015. Controls on nitrous oxide production and consumption in reservoirs of the Ohio River Basin. J. Geophys. Res.-Biogeo. 120(10), 1995–2010. https://doi.org/10.1002/2015JG002941.

Bowden, W.B., 1986. Nitrification, nitrate reduction, and nitrogen immobilization in a tidal freshwater marsh sediment. Ecology 67, 88–99. https://doi.org/10.2307/1938506.

Capodici, M., Avona, A., Laudicina, V.A., Viviani, G., 2018. Biological groundwater

denitrification systems: lab-scale trials aimed at nitrous oxide production and emission assessment. Sci. Total Environ. 630, 462–468. https://doi.org/10.1016/j.scitotenv.2018.02.260.

Chambers, L.G., Osborne, T.Z., Reddy, K.R., 2013. Effect of salinity-altering pulsing events on soil organic carbon loss along an intertidal wetlands gradient: a laboratory experiment. Biogeochemistry 115, 363–383. https://doi.org/10.1007/s10533-013-9841-5.

Cheng, X.L., Peng, R.H., Chen, J.Q., Luo, Y.Q., Zhang, Q.F., An, S.Q., Chen, J.K., Li, B., 2007. CH_4 and N_2O emissions from *Spartina alterniflora* and *Phragmites australis* in experimental mesocosms. Chemosphere 68(3), 420–427. https://doi.org/10.1016/j.chemosphere.2007.01.004.

Espenberg, M., Pille, K., Yang, B., Maddison, M., Abdalla, M., Smith, P., Li, X.Z., Chan, P. L., & Mander, Ü., 2024. Towards an integrated view on microbial CH_4, N_2O and N_2 cycles in brackish coastal marsh soils: A comparative analysis of two sites. Sci. Total Environ. 918, 170641. https://doi.org/10.1016/j.scitotenv.2024.170641.

Cloern, J.E., Abreu, P.C., Carstensen, J., Chauvaud, L., Elmgren, R., Grall, J., Greening, H., Johansson, J.O.R., Kahru, M., Sherwood, E.T., Xu, J., Yin, K., 2016. Human activities and climate variability drive fast-paced change across the world's estuarine-coastal ecosystems. Global Change Biol. 22 (2), 513–529. https://doi.org/10.1111/gcb.13059.

Chmura, G.L., Anisfeld, S.C., Cahoon, D.R., Lynch, J.C., 2003. Global carbon sequestration in tidal, saline wetland soils. Global Biogeochem. Cy. *17*(4), 1111. https://doi.org/10.1029/2002GB001917.

Comer-Warner, S.A., Nguyen, A.T.Q., Nguyen, M.N., Wang, M.L., Turner, A., Le,

H., Sgouridis, F., Krause, S., Kettridge, N., Nguyen, N., Liz Hamilton, R., Ullah, S., 2022. Restoration impacts on rates of denitrification and greenhouse gas fluxesfrom tropical coastal wetlands. Sci. Total Environ. 803, 149577. https://doi.org/10.1016/j.scitotenv.2021.149577.

Crusius, J., Wanninkhof, R., 2003. Gas transfer velocities measured at low wind speed over a lake. Limnol. Oceanogr. 48(3), 1010–1017.

Davidson, T.A., Audet, J., Svenning, J.-C., Lauridsen, T.L., Søndergaard, M., Landkildehus, F., Larsen, S.E., Jeppesen, E., 2015. Eutrophication effects on greenhouse gas fluxes from shallow-lake mesocosms override those of climate warming. Global Change Biol. 21, 4449–4463. https://doi.org/10.1111/gcb.13062.

Dinsmore, K.J., Billett, M.F., Dyson, K.E., 2013. Temperature and precipitation drive temporal variability in aquatic carbon and GHG concentrations and fluxes in a peatland catchment. Global Change Biol. 19, 2133–2148. https://doi.org/10.1111/gcb.12209.

Einola, E., Rantakari, M., Kankaala, P., Kortelainen, P., Ojala, A., Pajunen, H., Mäkelä, S., Arvola, L., 2011. Carbon pools and fluxes in a chain of five boreal lakes: a dry and wet year comparison. J Geophys Res.-Biogeosci 116, G03009. https://doi.org/10.1029/2010jg001636.

Ferrón, S., Ortega, T., Gómez-Parra, A., Forja, J.M., 2007. Seasonal study of dissolved CH_4, CO_2 and N_2O in a shallow tidal system of the bay of Cádiz (SW Spain). J. Marine Syst. 66, 244–257. https://doi.org/10.1016/j.jmarsys.2006.03.021.

Francis, C.A., O'Mullan, G.D., Ward, B.B., 2003. Diversity of ammonia monooxygenase (*amoA*) genes across environmental gradients in Chesapeake Bay sediments. Geobiology 1,

129–140. https://doi.org/10.1046/j.1472-4669.2003.00010.x.

Hama-Aziz, Z.Q., Hiscock, K.M., Cooper, R.J., 2017. Indirect nitrous oxide emission factors for agricultural field drains and headwater streams. Environ. Sci. Technol. 51, 301–307. https://doi.org/10.1021/acs.est.6b05094.

He, Y.X., Wang, X.F., Chen, H., Yuan, X.Z., Wu, N., Zhang, Y.W., Yue, J.S., Zhang, Q.Y., Diao, Y.B., Zhou, L.L., 2017. Effect of watershed urbanization on N_2O emissions from the Chongqing metropolitan river network, China. Atmos. Environ. 171, 70–81. https://doi.org/10.1016/j.atmosenv.2017.09.043.

Hinshaw, S.E., Dahlgren, R.A., 2013. Dissolved nitrous oxide concentrations and fluxes from the eutrophic San Joaquin River, California. Environ. Sci. Technol. 47, 1313–1322. https://doi.org/10.1021/es301373h.

Holgerson, M.A., 2015. Drivers of carbon dioxide and methane supersaturation in small, temporary ponds. Biogeochemistry 124(1–3), 305–318. https://doi.org/10.1007/s10533-015-0099-y.

Hosen, J.D., McDonough, O.T., Febria, C.M., Palmer, M.A., 2014. Dissolved organic matter quality and bioavailability changes across an urbanization gradient in headwater streams. Environ. Sci. Technol. 48, 7817-7824. https://doi.org/10.1021/es501422z.

Hu, M., Chen, D., Dahlgren, R.A., 2016. Modeling nitrous oxide emission from rivers: a global assessment. Global Change Biol. 22, 3566–3582. https://doi.org/10.1111/gcb.13351.

Huertas, I.E., Flecha, S., Navarro, G., Perez, F.F., de la Paz, M., 2018. Spatio-temporal variability and controls on methane and nitrous oxide in the Guadalquivir Estuary, Southwestern Europe. Aquat. Sci. 80(3), 29. https://doi.org/10.1007/s00027-018-0580-5.

Hutchins, D.A., Capone, D.G., 2022. The marine nitrogen cycle: new developments and global change. Nat. Rev. Microbiol. 20, 401–414. https://doi.org/10.1038/s41579-022-00687-z.

Kearney, W.S., Fagherazzi, S., 2016. Salt marsh vegetation promotes efficient tidal channel networks. tidal channel networks. Nat. Commun. 7, 12287. https://doi.org/10.1038/ncomms12287.

Kozlowski, J.A., Price, J., Stein, L.Y., 2014. Revision of N_2O-producing pathways in the ammonia-oxidizing bacterium Nitrosomonas europaea ATCC 19718. Appl. Environ. Microbiol. 80, 4930–4935. https://doi.org/10.1128/AEM.01061-14.

Laursen, A., Seitzinger, S., 2004. Diurnal patterns of denitrification, oxygen consumption and nitrous oxide production in rivers measured at the whole-reach scale. Freshwater Biol. 49(11), 1448–1458. https://doi.org/10.1111/j.1365-2427.2004.01280.x.

Li, X.F., Qi, M.T., Gao, D.Z., Liu, M., Sardans, J., Peñuelas, J., Hou, L.J., 2022. Nitrous oxide emissions from subtropical estuaries: Insights for environmental controls and implications. Water Res. 212, 118110. https://doi.org/10.1016/j.watres.2022.118110.

Li, X.F., Qian, W., Hou, L.J., Liu, M., Chen, Z.B., Tong, C., 2021. Human activity intensity controls the relative importance of denitrification and anaerobic ammonium oxidation across subtropical estuaries. Catena 202, 105260. https://doi.org/10.1016/j.catena.2021.105260.

Liang, J., Tang, W.Z., Zhu, Z.Q., Li, S., Wang, K., Gao, X., Li, X., Tang, N., Lu, L., Li, X.D., 2023. Spatiotemporal variability and controlling factors of indirect N_2O emission in a typical complex watershed. Water Res. 229, 119515. https://doi.org/10.1016/j.watres.2022.119515.

Liss, P.S., Slater, P.G., 1974. Flux of Gases across the Air-Sea Interface. Nature 247(5438), 181–184.

Liu, S.Y., Gao, Q.Z., Wu, J.X., Xie, Y.T., Yang, Q.Q., Wang, R.W., Zhang, J., Liu, Q., 2022. Spatial distribution and influencing mechanism of CO_2, N_2O and CH_4 in the Pearl River Estuary in summer. Sci. Total Environ. 846, 157381. https://doi.org/10.1016/j.scitotenv.2022.157381

Lu, Z.Y., Wang, F.F., Xiao, K., Wang, Y., Yu, Q.B., Cheng, P., Chen, N.W., 2023. Carbon dynamics and greenhouse gas outgassing in an estuarine mangrove wetland with high input of riverine nitrogen. Biogeochemistry 162, 221–235. https://doi.org/10.1007/s10533-022-00999-5.

Ma, J.J., Niu, A.Y., Liao, Z.N., Qin, J.H., Xu, S.J., Lin, C.X., 2023. Factors affecting N_2O fluxes from heavy metal-contaminated mangrovesoils in a subtropical estuary. Mar. Pollut. Bull. 186, 114425. https://doi.org/10.1016/j.marpolbul.2022.114425.

Maher, D.T., Sippo, J.Z., Tait, D.R., Holloway, C., Santos, I.R., 2016. Pristine mangrove creek waters are a sink of nitrous oxide. Sci. Rep. 6, 25701. https://doi.org/10.1038/srep25701.

Murray, R.H., Erler, D.V., Eyre, B.D., 2015. Nitrous oxide fluxes in estuarine environments: response to global change. Global Change Biol. 21(9), 3219–3245. https://doi.org/10.1111/gcb.12923.

Murray, R.H., Erler, D.V., Rosentreter, J., Maher, D., Bradley, E., 2018. A seasonal source and sink of nitrous oxide in mangroves: insights from concentration, isotope, and isotopomer measurements. Geochim. Cosmochim. Ac. 238, 169–192. https://doi.org/10.1016/j.gca.2018.07.003.

Musenze, R.S., Grinham, A., Werner, U., Gale, D., Sturm, K., Udy, J., Yuan, Z.G., 2014. Assessing the spatial and temporal variability of diffusive methane and nitrous oxide emissions from subtropical freshwater reservoirs. Environ. Sci. Technol. 48, 14499–14507. https://doi.org/10.1021/es505324h.

Natchimuthu, S., Panneer Selvam, B., Bastviken, D., 2014. Influence of weather variables on methane and carbon dioxide flux from a shallow pond. Biogeochemistry 119, 403–413. https://doi.org/10.1007/s10533-014-9976-z.

Neubauer, S.C., Franklin, R.B., Berrier, D.J., 2013. Saltwater intrusion into tidal freshwater marshes alters the biogeochemical processing of organic carbon. Biogeosciences 10, 8171–8183. https://doi.org/10.5194/bg-10-8171-2013.

Outram, F.N., Hiscock, K.M., 2012. Indirect nitrous oxide emissions from surface water bodies in a lowland arable catchment: a significant contribution to agricultural greenhouse gas budgets? Environ. Sci. Technol. 46, 8156–8163. https://doi.org/10.1021/es3012244.

Prosser, J.I., Hink, L., Gubry-Rangin, C., Nicol, G.W., 2020. Nitrous oxide production by ammonia oxidisers: Physiological diversity, niche differentiation and potential mitigation strategies. Global Change Biol. 26, 103–118. https://doi.org/10.1111/gcb.14877.

Pieterse, A., Puleo, J.A., McKenna, T.E., 2016. Hydrodynamics and sediment suspension in shallow tidal channels intersecting a tidal flat. Cont. Shelf Res. 119, 40–55. https://doi.org/10.1016/j.csr.2016.03.012.

Plummer, P., Tobias, C., Cady, D., 2015. Nitrogen reduction pathways in estuarine sediments: Influences of organic carbon and sulfide. J. Geophys. Res.: Biogeosciences 120(10), 1958–1972. https://doi.org/10.1002/2015JG003057.

Que, Z.Y., Wang, X.F., Liu, T.T., Wu, S.N., He, Y.X., Zhou, T., Yu, L.L., Qing, Z.Y., Chen, H., Yuan, X.Z., 2023. Watershed land use change indirectly dominated the spatial variations of CH_4 and N_2O emissions from two small suburban rivers. J. Hydrol. 619, 129357. https://doi.org/10.1016/j.jhydrol.2023.129357.

Ravishankara, A.R., Daniel, J., Portmann, R., 2009. Nitrous Oxide (N_2O): the dominant ozone-depleting substance emitted in the 21st Century. Science 326, 123–125. https://doi.org/10.1126/science.1176985.

Raymond, P.A., Cole, J.J., 2001. Gas exchange in rivers and estuaries: choosing a gas transfer velocity. Estuaries 24, 312–317. https://doi.org/10.2307/1352954.

Rysgaard, S., Thastum, P., Dalsgaard, T., Christensen, P.B., Sloth, N.P., 1999. Effects of salinity on NH_4^+ adsorption capacity, nitrification, and denitrification in Danish estuarine sediments. Estuar. Coast. 22, 21–30.

Sanderson, E.W., Ustin, S.L., Foin, T.C., 2000. The influence of tidal channels on the distribution of salt marsh plant species in Petaluma Marsh, CA, USA. Plant Ecol. 146, 29–41. https://doi.org/10.1023/A:1009882110988.

Sanger, D., Blair, A., DiDonato, G., Washburn, T., Jones, S., Riekerk, G., Wirth, E., Stewart, J., White, D., Vandiver, L., Holland, A.F., 2015. Impacts of coastal development on the ecology of tidal creek ecosystems of the US southeast including consequences to humans. Estuar. Coast. 38(Suppl 1), 49–66. https://doi.org/10.1007/s12237-013-9635-y.

Sinha, E., Michalak, A.M., Balaji, V., 2017. Eutrophication will increase during the 21st century as a result of precipitation changes. Science 357, 405–408. https://doi.org/10.1126/science.aan2409.

Shen, L.D., Hu, B.L., Liu, S., Chai, X.P., He, Z.F., Ren, H.X., Liu, Y., Geng, S., Wang, W., Tang, J.L., Wang, Y.M., Lou, L.P., Xu, X.Y., 2016. Anaerobic methane oxidation coupled to nitrite reduction can be a potential methane sink in coastal environments. Appl. Microbiol. Biot. 100, 7171–7180. https://doi.org/10.1007/s00253-016-7627-0.

Shrestha, N.K., Wang, J., 2018. Current and future hot-spots and hot-moments of nitrous oxide emission in a cold climate river basin. Environ. Pollut. 239, 648–660. https://doi.org/10.1016/j.envpol.2018.04.068.

Schulz, G., Sanders, T., Voynova, Y.G., Bange, H.W., Dähnke, K., 2023. Seasonal variability of nitrous oxide concentrations and emissions in a temperate estuary. Biogeosciences 20, 3229–3247. https://doi.org/10.5194/bg-20-3229-2023.

Stanley, E.H., Casson, N.J., Christel, S.T., Crawford, J.T., Loken, L.C., Oliver, S.K., 2016. The ecology of methane in streams and rivers: patterns, controls, and global significance. Ecol. Monogr. 86, 146–171. https://doi.org/10.1890/15-1027.

Sturm, K., Werner, U., Grinham, A., Yuan, Z.G., 2017. Tidal variability in methane and nitrous oxide emissions along a subtropical estuarine gradient. Estuar. Coast. Shelf S. 192, 159–169. https://doi.org/10.1016/j.ecss.2017.04.027.

Tan, L.S., Ge, Z.M., Li, S.H., Li, Y.L., Xie, L.N., Tang, J.W., 2021. Reclamation-induced tidal restriction increases dissolved carbon and greenhouse gases diffusive fluxes in salt marsh creeks. Sci. Total Environ. 773, 145684. https://doi.org/10.1016/j.scitotenv.2021.145684.

Tian, H.Q., Xu, R.T., Canadell, J.G., Thompson, R.L., Winiwarter, W., Suntharalingam, P., Davidson, E.A., Ciais, P., Jackson, R.B., Janssens-Maenhout, G., Prather, M.J., Regnier, P., Pan, N.Q., Pan, S.F., Peters, G.P., Shi, H., Tubiello, F.N., Zaehle, S., Zhou, F., Arneth, A., Battaglia,

G., Berthet, S., Bopp, L., Bouwman, A.F., Buitenhuis, E.T., Chang, J.F., Chipperfield, M.P., Dangal, S.R.S., Dlugokencky, E., Elkins, J.W., Eyre, B.D., Fu, B.J., Hall, B., Ito, A., Joos, F., Krummel, P.B., Landolfi, A., Laruelle, G.G., Lauerwald, R., Li, W., Lienert, S., Maavara, T., MacLeod, M., Millet, D.B., Olin, S., Patra, P.K., Prinn, R.G., Raymond, P.A., Ruiz, D.J., van der Werf, G.R., Vuichard, N., Wang, J.J., Weiss, R.F., Wells, K.C., Wilson, C., Yang, J., Yao, Y.Z., 2020. A comprehensive quantification of global nitrous oxide sources and sinks. Nature 586, 248–255. https://doi.org/10.1038/s41586-020-2780-0.

Tian, L.L., Zhu, B., Akiyama, H., 2017. Seasonal variations in indirect N_2O emissions from an agricultural headwater ditch. Biol. Fert. Soils 53, 651–662. https://doi.org/10.1007/s00374-017-1207-z.

Toyoda, S., Yano, M., Nishimura, S.I., Akiyama, H., Hayakawa, A., Koba, K., Ogawa, N.O., 2011. Characterization and production and consumption processes of N_2O emitted from temperate agricultural soils determined via isotopomer ratio analysis. Global Biogeochem. Cy. 25, 96–101. https://doi.org/10.1029/2009GB003769.

Vandenbruwaene, W., Meire, P., Temmerman, S., 2012. Formation and evolution of a tidal channelnetwork within a constructed tidal marsh. Geomorphology 151–152. https://doi.org/10.1016/j.geomorph.2012.01.022.

Venterea, R.T., 2007. Nitrite-driven nitrous oxide production under aerobic soil conditions: Kinetics and biochemical controls. Global Change Biol. 13(8), 1798–1809. https://doi.org/10.1111/j.1365-2486.2007.01389.x.

Wang, H.T., Liao, G.S., D'Souza, M., Yu, X.Q., Yang, J., Yang, X.R., Zheng, T.L., 2015. Temporal and spatial variations of greenhouse gas fluxesfrom a tidal mangrove wetland in

Southeast China. Environ. Sci. Pollut. R. 23(2), 1873–1885. https://doi.org/10.1007/s11356-015-5440-4.

Wang, R., Zhang, H., Zhang, W., Zheng, X.H., Butterbach-Bahl, K., Li, S.Q., Han, S.H., 2020. An urban polluted river as a significant hotspot for water–atmosphere exchange of CH_4 and N_2O. Environ. Pollut. 264, 114770 https://doi.org/10.1016/j.envpol.2020.114770.

Wang, X.M., Hu, M.J., Ren, H.C., Li, J.B., Tong, C., Musenze, R.S., 2018. Seasonal variations of nitrous oxide fluxes and soil denitrification rates in subtropical freshwater and brackish tidal marshes of the Min River estuary. Sci. Total Environ. 616-617, 1404–1413. https://doi.org/10.1016/j.scitotenv.2017.10.175.

Wang, Z.Y., Xin, Y.Z., Gao, D.M., Li, F.M., Morgan, J., Xing, B.S., 2010. Microbial community characteristics in a degraded wetland of the Yellow River Delta. Pedosphere 20(4), 466–478. https://doi.org/10.1016/S1002-0160(10)60036-7.

Wanninkhof, R., 1992. Relationship between wind speed and gas exchange over the ocean. J. Geophys. Res. 97(C5), 7373–7382. https://doi.org/10.1029/92jc00188.

Weiss, R.F., Price, B.A., 1980. Nitrous oxide solubility in water and seawater. Mar. Chem. 8(4), 347–359. https://doi.org/10.1016/0304-4203(80)90024-9.

Wells, N. S., Maher, D. T., Erler, D. V., Hipsey, M., Rosentreter, J. A., Eyre, B. D., 2018. Estuaries as sources and sinks of N_2O across a land use gradient in subtropical Australia. Global Biogeochem. Cy. 32(5), 877–894. https://doi.org/10.1029/2017gb005826.

Wessel, M.R., Leverone, J.R., Beck, M.W., Sherwood, E.T., Hecker, J., West, S., Janicki, A., 2022. Developing a water quality assessment framework for southwest Florida tidal creeks. Estuar. Coast. 45, 17–37. https://doi.org/10.1007/s12237-021-00974-7.

WMO, 2023. The state of greenhouse gases in the atmosphere based on global observations through 2022. World Meteorological Organization, WMO Greenhouse Gas Bulletin (GHG Bulletin), Issue No. 19.

Wu, Y.A., Liu, J.K., Yan, G.X., Zhai, J.X., Cong, L., Dai, L.Y., Zhang, Z.M., Zhang, M.X., 2020. The size and distribution of tidal creeks affects salt marsh restoration. J. Environ. Manage. 259, 110070. https://doi.org/10.1016/j.jenvman.2020.110070.

Xiang, H., Hong, Y.G., Wu, J.P., Wang, Y., Ye, F., Hu, Z., Qu, Z.M., Long, A.M., 2023. NosZ–II–type N_2O-reducing bacteria play dominant roles in determining the release potential of N_2O from sediments in the Pearl River Estuary, China. Environ. Pollut. 329, 121732. https://doi.org/10.1016/j.envpol.2023.121732.

Xiao, Q.T., Xu, X.F., Zhang, M., Duan, H.T., Hu, Z.H., Wang, W., Xiao, W., Lee, X.H., 2019a. Coregulation of nitrous oxide emissions by nitrogen and temperature in China's third largest freshwater lake (Lake Taihu). Limnol. Oceanogr. 64, 1070–1086. http://dx.doi.org/10.1002/lno.11098.

Xiao, Q.T., Hu, Z.H., Fu, C.S., Bian, H., Lee, X.H., Chen, S.T., Shang, D.Y., 2019b. Surface nitrous oxide concentrations and fluxes from water bodies of the agricultural watershed in Eastern China. Environ. Pollut. 251, 185–192. http://dx.doi.org/10.1016/j.envpol.2019.04.076.

Xiao, Q.T., Hu, Z.H., Hu, C., Towfiqul Islam, A.R.M., Bian, H., Chen, S.T., Liu, C., Lee, X.H., 2021. A highly agricultural river network in Jurong Reservoir watershed as significant CO_2 and CH_4 sources. Sci. Total Environ. 769, 144558. https://doi.org/10.1016/j.scitotenv.2020.144558.

Yang, P., Tang, K.W., Zhang, L.H., Lin, X., Yang, H., Tong, C., Hong, Y., Tan, L.S., Lai, D.Y.F., Tian, Y.L., Zhu, W.Y., Ruan, M.J., Lin, Y.X., 2023. Effects of landscape modification on coastal sediment nitrogen availability, microbial functional gene abundances and N_2O production potential across the tropical-subtropical gradient. Environ. Res. 227, 115829. https://doi.org/10.1016/j.envres.2023.115829.

Yang, P., Huang, J.F., Tan, L.S., Tong, C., Jin, B.S., Hu, B.B., Gao, C.J., Yuan, J.J., Lai, D.Y.F., Yang, H., 2021a. Large variations in indirect N_2O emission factors (EF_5) from coastal aquaculture systems in China from plot to regional scales. Water Res. 200, 117208. https://doi.org/10.1016/j.watres.2021.117208.

Yang, P., Lu, M., Tang, K.W., Yang, H., Lai, D.Y.F., Tong, C., Chun, K.P., Zhang, L.H., Tang, C., 2021b. Coastal reservoirs as a source of nitrous oxide: Spatio-temporal patterns and assessment strategy. Sci. Total Environ. 790, 147878. https://doi.org/10.1016/j.scitotenv.2021.147878

Yang, P., Luo, L.J., Tang, K.W., Lai, D.Y.F., Tong, C., Hong, Y., Zhang, L.H., 2022a. Environmental drivers of nitrous oxide emission factor for a coastal reservoir and its catchment areas in southeastern China. Environ. Pollut. 294, 118568. https://doi.org/10.1016/j.envpol.2021.118568.

Yang, P., Tang, K.W., Tong, C., Lai, D.Y.F., Zhang, L.H., Lin, X., Yang, H., Tan, L.S., Zhang, Y.F., Hong, Y., Tang, C., Lin, Y.X., 2022b. Conversion of coastal wetland to aquaculture ponds decreased N_2O emission: Evidence from a multi-year field study. Water Res. 227, 119326. https://doi.org/10.1016/j.watres.2022.119326

Yu, Z.J., Wang, D.Q., Li, Y.J., Deng, H.G., Hu, B.B., Ye, M.W., Zhou, X.H., Da, L.J., Chen,

Z.L., Xu, S.Y., 2017. Carbon dioxide and methane dynamics in a human-dominated lowland coastal river network (Shanghai, China). J. Geophys. Res.-Biogeo. 122(7), 1738–1758. https://doi.org/10.1002/2017JG003798.

Zhang, S.B., Xia, X.H., Xin, Y., Li, X.K., Wang, J.F., Yu, L.L., Li, C.B., McDowell, W.H., Tan, Q., Yang, Z.F., 2023. Electrical conductivity as a reliable indicator for assessing land use effects on stream N_2O concentration. J. Hydrol. 626, 130253. https://doi.org/10.1016/j.jhydrol.2023.130253.

Zhang, Y.H., Xu, X.J., Li, Y., Huang, L.D., Xie, X.J., Dong, J.M., Yang, S.Q., 2016. Effects of *Spartina alterniflora* invasion and exogenous nitrogen on soil nitrogen mineralization in the coastal salt marshes. Ecol. Eng. 87, 281–287. http://dx.doi.org/10.1016/j.ecoleng.2015.12.003.

Zhou, J., Zheng, Y,L., Hou, L.J., An, Z.R., Chen, F.Y., Liu, B.L., Wu, L., Qi, L., Dong, H.P., Han, P., Yin, G.Y., Liang, X., Yang, Y., Li, X.F., Gao, D.Z., Li, Y., Liu, Z.F., Bellerby, R., Liu, M., 2023. Effects of acidification on nitrification and associated nitrous oxide emission in estuarine and coastal waters. Nat. Commun. 14, 1380. https://doi.org/10.1038/s41467-023-37104-9.

Zhu, X., Burger, M., Doane, T.A., Horwath, W.R., 2013. Ammonia oxidation pathways and nitrifier denitrification are significant sources of N_2O and NO under low oxygen availability. PNAS 110(16), 6328–6333. https://doi.org/10.1073/pnas.1219993110

Table 1

Summary of ANOVAs examining the seasonal effect on nitrogenous substrate in the surface water at a coastal creek in the Shanyutan Wetland, southeastern China. Within each column, different letters indicate significant differences (p<0.05) between seasons.

Seasons	Nitrogenous substrate (mg L^{-1})		
	TN	NO_3^--N	NH_4^+-N
Autumn	2.81±0.31a	1.46±0.05a	1.35±0.26a
Winter	1.84±0.05bc	0.94±0.03c	0.56±0.05b
Spring	2.12±0.07b	1.24±0.01b	0.76±0.05b
Summer	1.62±0.10c	0.84±0.05c	0.44±0.04b

Table 2

Summary of non-parametric methods examining the seasonal effect on microbial functional gene abundances in the surface water at a coastal creek in the Shanyutan Wetland, southeastern China. Within each column, different letters indicate significant differences (p<0.05) between seasons.

Seasons	Microbial functional gene abundances (copies L^{-1})					
	AOA *amoA* (× 10^5)	AOB *amoA* (× 10^7)	*nirK* (× 10^7)	*nirS* (× 10^7)	*nosZ* I (× 10^9)	*nosZ* II (× 10^7)
Autumn	4.18±0.29a	4.13±0.31a	34.3±3.93a	25.2±4.04a	6.17±0.42a	4.18±0.47a
Winter	2.52±0.18b	3.14±0.23b	17.2±2.60b	12.8±1.52b	4.86±0.39b	2.57±0.29b
Spring	3.00±0.39b	2.26±0.13c	6.47±0.29c	6.64±0.31c	0.39±0.02c	2.47±0.17b
Summer	3.17±0.20b	2.63±0.21bc	6.56±0.82c	9.09±0.75bc	0.42±0.05c	3.57±0.26a

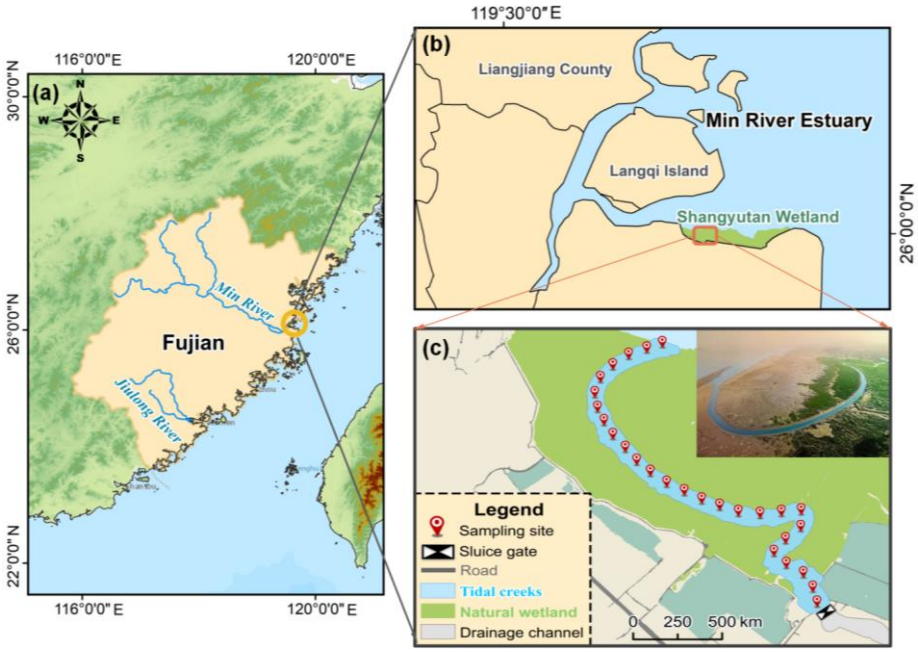

Figure 1. Map of study area in southeastern China (a) showing the coastal creek within the Shanyutan Wetland (b) and the sampling sites (c).

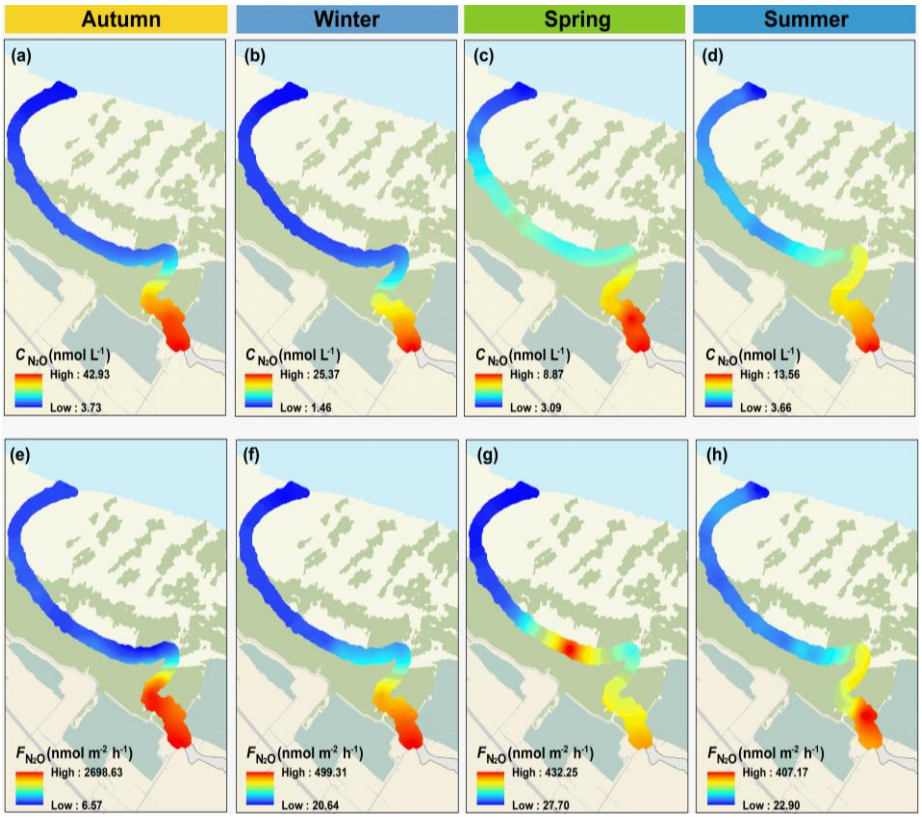

Figure 2. Spatial distributions of surface-water dissolved N_2O concentration (C_{N2O}; a-d) and water-to-air diffusive N_2O flux (F_{N2O}; e-h) in different seasons along the coastal creek in the Shanyutan Wetland, southeastern China.

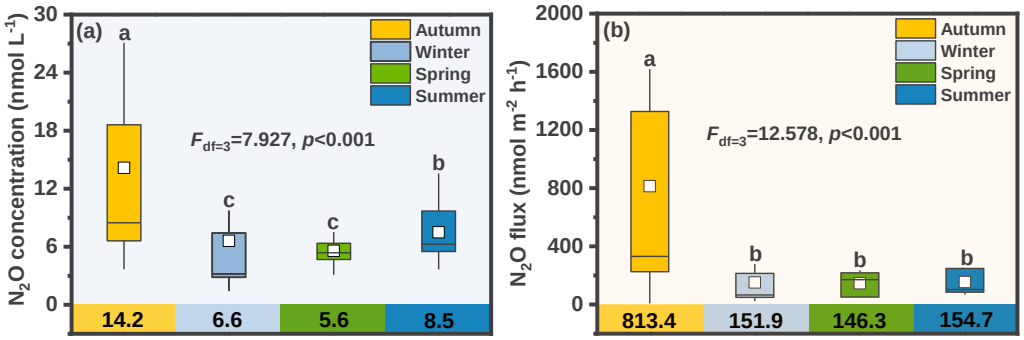

Figure 3. Box plots of seasonal data for (a) dissolved N_2O concentration and (b) water-to-air diffusive N_2O flux in the coastal creek. The boxes, square, and whiskers represent the 25^{th}–75^{th} percentiles, mean and standard deviations, respectively. Number underneath each box is the seasonal mean value. Different letters above the boxes indicate significant differences between seasons (p<0.05).

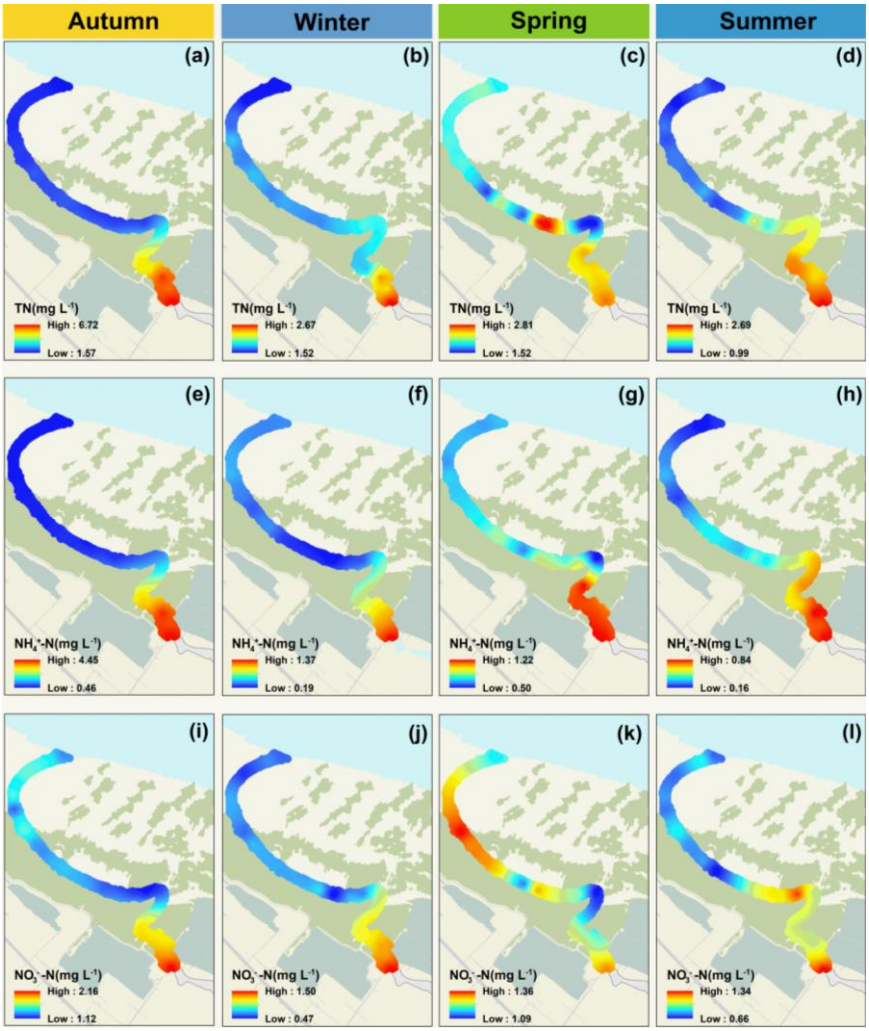

Figure 4. Spatial distributions of nitrogenous substrates: TN (a-d), NH_4^+-N (e-h) and NO_3^--N (i-l) in the surface water of the coastal creek in the Shanyutan wetland, southeastern China.

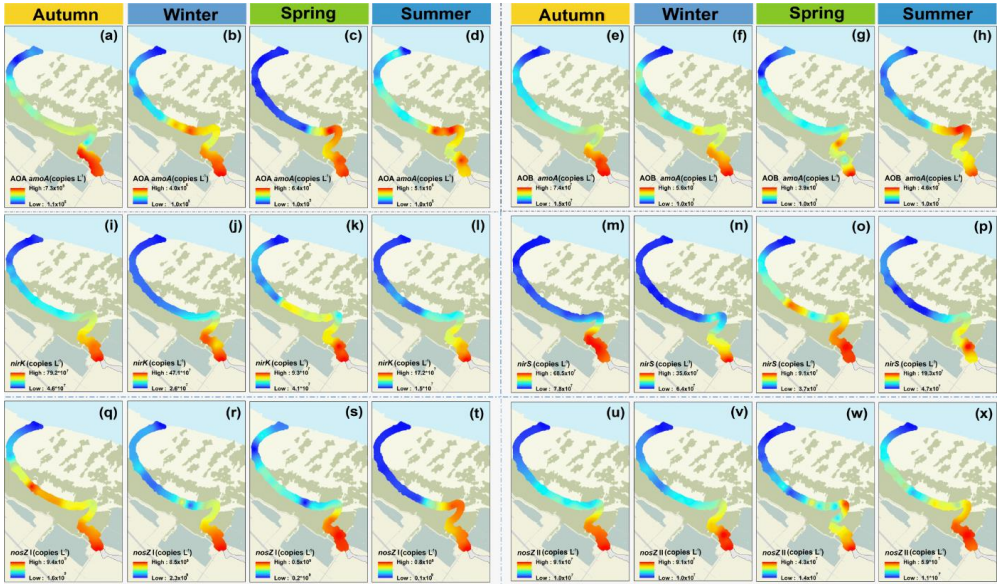

Figure 5. Spatial distributions of gene abundances: AOA *amoA* (a-d), AOB *amoA* (e-h), *nirK* (i-l), *nirS* (m-p), *nosZ* I (q-t) and *nosZ* II (u-x) in the surface water of the coastal creek in the Shanyutan Wetland, southeastern China.

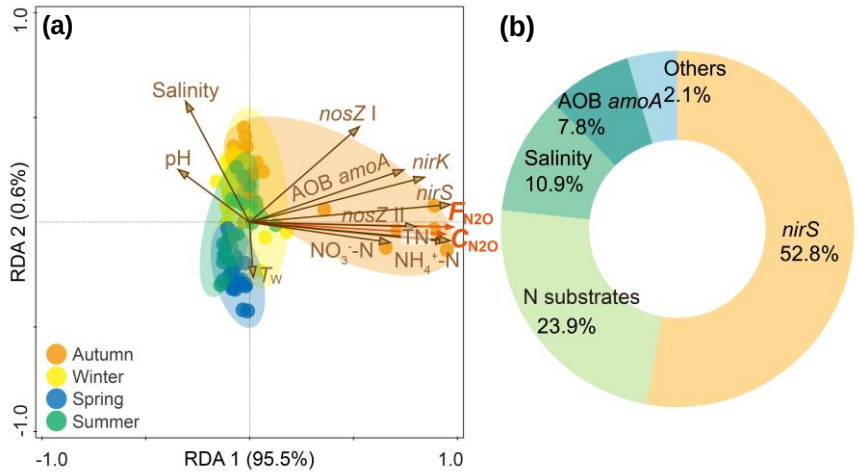

Figure 6. Results of redundancy analysis (RDA) between dissolved N_2O concentration (C_{N2O}), diffusive N_2O flux (F_{N2O}) and environmental variables (a). The pie chart (b) shows the percentages of variance in C_{N2O} and F_{N2O} explained by the different variables.

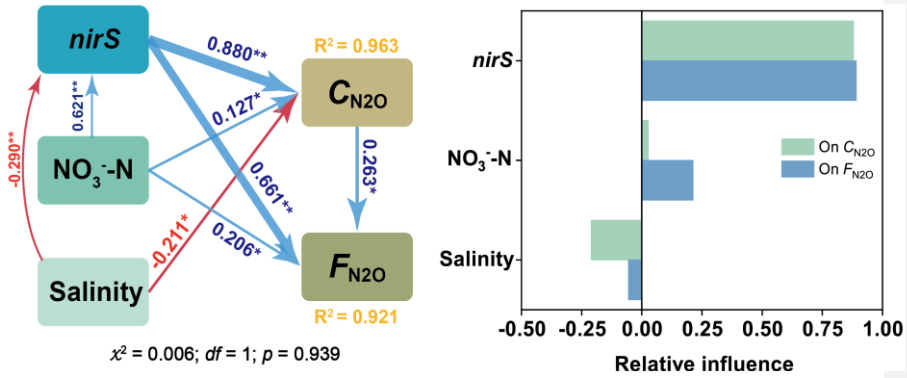

Figure 7. Partial least square structural equation modeling (PLS-SEM) assessing the direct and indirect effects of environmental variables on dissolved N_2O concentration (C_{N2O}) and N_2O diffusive flux (F_{N2O}). Blue and red arrows indicate significantly positive and negative effects, respectively. Numbers adjacent to the arrows are standardized path coefficients indicating the effect size of the relationships. R^2 represents the variance explained for the target variables. Bar graph shows the relative influence of the environmental variables on C_{N2O} and F_{N2O}. * $p < 0.05$; ** $p < 0.01$.

Supporting Information

Spatiotemporal distributions of dissolved N_2O concentration, diffusive N_2O flux and relevant functional genes along a coastal creek in southeastern China

Ping Yang[a,b,c,d*], Yongxin Lin[a,b], Hong Yang[e], Chuan Tong[a,c,d], Linhai Zhang[a,b,c,d], Derrick Y. F. Lai[f], Dongyao Sun[g*], Lishan Tan[f], Lele Tang[a], Yan Hong[a], Kam W. Tang[g*]

[a]*School of Geographical Sciences, Fujian Normal University, Fuzhou 350007, P.R. China*

[b]*Fujian Provincial Key Laboratory for Subtropical Resources and Environment, Fujian Normal University, Fuzhou 350117, P.R. China*

[c]*Research Centre of Wetlands in Subtropical Region, Fujian Normal University, Fuzhou 350007, P.R. China*

[d]*Fujian Minjiang Estuary Wetland Ecosystem National Observation and Research Station, National Forestry and Grassland Administration, Fuzhou 350215, China*

[e]*Department of Geography and Environmental Science, University of Reading, Reading, UK*

[f]*Department of Geography and Resource Management, The Chinese University of Hong Kong, Shatin, New Territories, Hong Kong SAR, China*

[g]*School of Geography Science and Geomatics Engineering, Suzhou University of Science and Technology, Suzhou 215009, China*

[h]*Department of Biosciences, Swansea University, Swansea SA2 8PP, U. K.*

***Corresponding author:**

yangping528@sina.cn (P. Yang); dongyaos@126.com (D.Y. Sun); k.w.tang@swansea.ac.uk (K.W. Tang)

Supporting Information Summary

No. of pages: 7 **No. of figures:** 3 **No. of tables:** 2

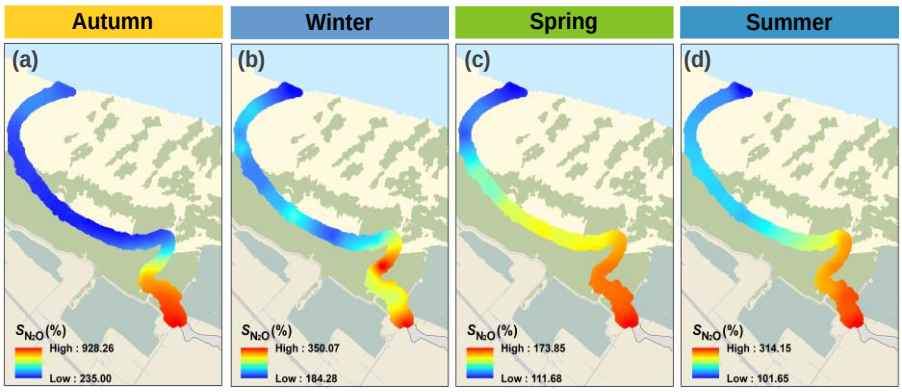

74

75 **Figure S1** Spatial distributions of surface-water N_2O % saturation (S_{N2O}) in the coastal creek in the

76 Shanyutan Wetland, southeastern China.

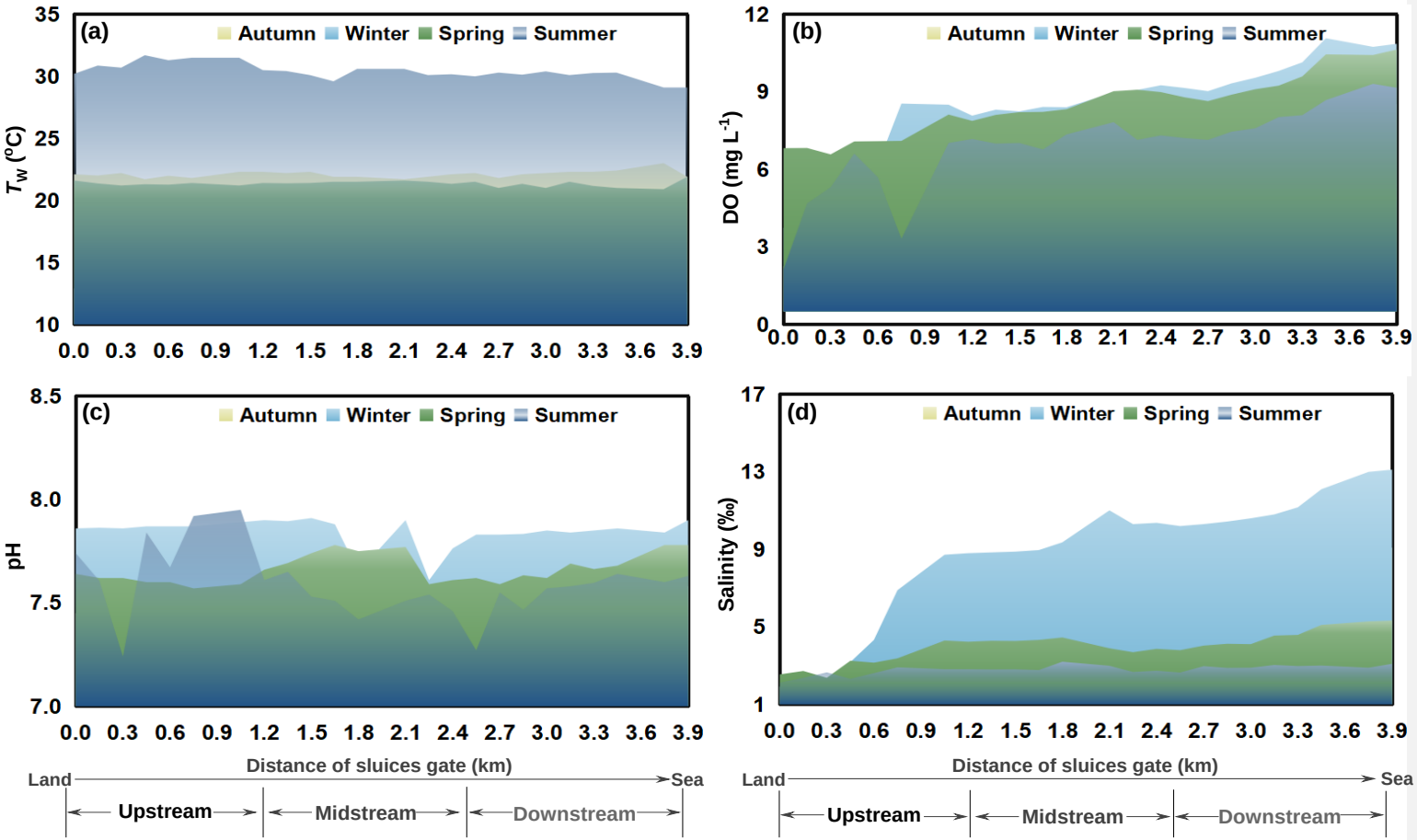

Figure S2 Spatial distributions of surface-water temperature (*T*w; a), dissolved oxygen (DO, b), salinity (c) and pH (d) in the coastal creek in the Shanyutan

Wetland, southeastern China. Data are after Yang et al. [unpublish] for reference and review only.

Commented [KT3]: Dr Yang, do you intend to remove it from the final (published) version? Because the environmental data are a key part of the data analysis and Figure S2 is mentioned multiple times in the text, I think it is necessary to keep this figure in the final (published) version.

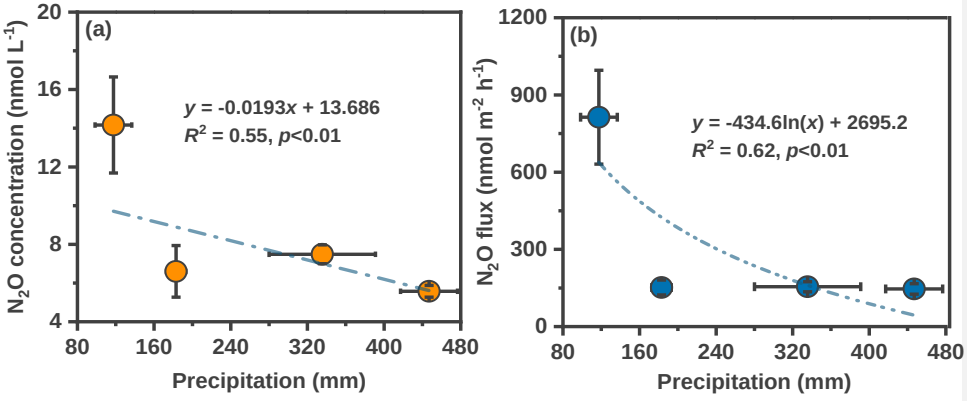

Figure S3 Relationship between dissolved N_2O concentration, diffusive N_2O flux and precipitation in the coastal creek in the Shanyutan Wetland, southeastern China. N_2O concentration and flux data are from this study; precipitation data are taken from the Min River Estuary weather station as a part of the China Wetland Ecosystem Research Network.

Table S1

PCR primers and thermal cycling conditions used for gene quantification.

Gene	Primer	Sequence	Thermal conditions	References
AOA *amoA*	Arch-*amoA*F	STAATGGTCTGGCTTAGACG	95°C, 3min；35×（95°C for 10 s, 55°C for 30 s, 72°C for 45 s+ plate read）；Melt curve：65.0°C to 95.0°C, increment 0.5°C, 0:05+ plate read	Francis et al., 2005
	Arch-*amoA*R	GCGGCCATCCATCTGTAT GT		
AOB *amoA*	amoA-1F	GGGGTTTCTACTGGTGGT	95°C, 3min；35×（95°C for 10 s, 55°C for 30 s, 72°C for 45 s+ plate read）；Melt curve：65.0°C to 95.0°C, increment 0.5°C, 0:05+ plate read	Rotthauwe et al., 1997
	amoA-2R	CCC CTC KGS AAA GCCTTCTTC		
nirS	nirSCd3aF	GTSAACGTSAAGGARACSGG	95°C, 3 min；35×（95°C for 10 s, 56 °C for 30 s, 72°C for 20 s+ plate read）；Melt curve：65.0°C to 95.0°C, increment 0.5°C, 0:05+ plate read	Throbäck et al., 2004
	nirSR3cd	GASTTCGGRTGSGTCTTGA		
nirK	nirKF1aCu	ATCATGGTSCTGCCGCG	95°C, 3 min；35×（95°C for 10 s, 56 °C for 30 s, 72°C	Throbäck et al., 2004

	nirKR3Cu	GCCTCGATCAGRTTGTGGTT	for 20 s+ plate read）；Melt curve：65.0°C to 95.0°C, increment 0.5°C, 0:05+ plate read	
***nosZ* I**	nosZ1840F	CGCRACGGCAASAAGGTSMSSGT	95°C, 3 min；35×（95°C for 10 s, 58 °C for 25 s, 72°C for 20 s+ plate read）；Melt curve：65.0°C to 95.0°C, increment 0.5°C, 0:05+ plate read	Henry et al., 2006
	nosZ2090R	CAKRTGCAKSGCRTGGCAGAA		
***nosZ* II**	nosZ-II-F	CTIGGICCIYTKCAYAC	95°C, 3 min；35×（95°C for 10 s, 54 °C for 30 s, 72°C for 40 s+ plate read）；Melt curve：65.0°C to 95.0°C, increment 0.5°C, 0:05+ plate read	Jones et al., 2013
	nosZ-II-R	GCIGARCARAAITCBGTRC		

87

Table S2

Spearman correlation coefficients between dissolved N_2O concentration (C_{N2O}), diffusive N_2O flux (F_{N2O}) and environmental variables for the coastal creek in the Shanyutan Wetland, southeastern China. The symbols * and ** denote significant correlations at $p < 0.05$ and $p < 0.01$, respectively. T_W, DO and TN represent water temperature, dissolved oxygen and total dissolved nitrogen, respectively.

					Nitrogenous substrates			N_2O-related functional gene abundances					
	T_W	DO	pH	salinity	TN	NO_3^--N	NH_4^+-N	AOA *amoA*	AOB *amoA*	*nirK*	*nirS*	*nosZ* I	*nosZ* II
C_{N2O}	0.478**	-0.921**	-0.361	-0.744**	0.594**	0.514**	0.654**	0.752**	0.709**	0.604**	0.692**	0.350**	0.918**
F_{N2O}	0.300**	-0.797**	-0.242	-0.455**	0.632**	0.602**	0.656**	0.735**	0.738**	0.748**	0.777**	0.526**	0.757**

References

Francis, C.A., Roberts, K.J., Beman, J.M., Santoro, A.E., Oakley, B.B., 2005. Ubiquity and diversity of ammonia oxidizing archaea in water columns and sediments of the ocean. P. Natl. Acad. Sci. USA 102, 14683–14688. https://doi.org/10.1073/pnas.0506625102

Henry, S., Bru, D., Stres, B., Hallet, S., Philippot, L., 2006. Quantitative detection of the *nosZ* gene, encoding nitrous oxide reductase, and comparison of the abundances of 16S rRNA, *narG*, *nirK*, and *nosZ* genes in soils. Appl. Environ. Microb. 72, 5181–5189. https://doi.org/10.1128/AEM.00231-06

Jones, C.M., Graf, D.R.H., Bru, D., Philippot, L., Hallin, S., 2013. The unaccounted yet abundant nitrous oxide-reducing microbial community: a potential nitrous oxide sink. ISME J. 7, 417–426. https://doi.org/10.1038/ismej.2012.125

Rotthauwe, J.H., Witzel, K.P., Liesack, W., 1997. The ammonia monooxygenase structural gene amoA as a functional marker: molecular fine-scale analysis of natural ammonia-oxidizing populations. Appl. Environ. Microb. 63, 4704–4712. https://doi.org/10.1128/aem.63.12.4704-4712.1997

Throbäck, I.N., Enwall, K., Jarvis, Å., Hallin, S., 2004. Reassessing PCR primers targeting *nirS*, *nirK* and *nosZ* genes for community surveys of denitrifying bacteria with DGGE. FEMS Microbiol. Ecol. 49, 401–417. https://doi.org/10.1016/j.femsec.2004.04.011